Wigner defects bridge the graphite gap

ROB H. TELLING*, CHRIS P. EWELS[†], AHLAM A. EL-BARBARY AND MALCOLM I. HEGGIE

The University of Sussex, Falmer, Brighton BN1 9QJ, UK
[†]Present address: DMSC, ONERA, 29 Avenue de la Division Leclerc, 92322 Chatillon, France
*e-mail: r.h.telling@sussex.ac.uk

We present findings on the structure, energies and behaviour of defects in irradiated graphitic carbon materials. Defect production due to high-energy nuclear radiations experienced in graphite moderators is generally associated with undesirable changes in internal energy, microstructure and physical properties—the so-called Wigner effect. On the flip side, the controlled introduction and ability to handle such defects in the electron beam is considered a desirable way to engineer the properties of carbon nanostructures. In both cases, the atomic-level details of structure and interaction are only just beginning to be understood. Here, using a model system of crystalline graphite, we show from first-principles calculations, new details in the behaviour of vacancy and interstitial defects. We identify a prominent barrier-state to energy release, reveal a surprising ability of vacancy defects to bridge the widely spaced atomic layers, and discuss physical property and microstructure changes during irradiation, including interactions with dislocations.

Radiation effects in carbon materials have received considerable attention over the years, particularly the damaging effects of neutrons on graphite in a nuclear reactor[1]. This interest originally stemmed from problems associated with fission reactor operations, for example, dimensional changes and defect rearrangements leading to spontaneous release of energy—an effect implicated in the Windscale reactor fire[2] of 1957. More recently, fundamental studies of the defect physics in graphite have been undertaken to assess safety aspects concerning reactor decommissioning, and as model systems for defects in more complex carbon materials. These include the graphitic-based structures being investigated in nanoscience research fields, where the focus is not so much on damage, but on engineering favourable structural and/or electronic properties through electron irradiation[3]. In all these cases, to achieve the best understanding of the behaviour of the system, defect structure and energetics must be examined using a full quantum-mechanical treatment.

In irradiated graphite, a generally complex defect population evolves over many different length scales[4]. There is still scant information of a basic nature as to what these defects are and how they interact. Similarly, there are major gaps in understanding their effect on physical properties and microstructure, still largely understood only at a phenomenological level. We aim here to derive a deeper understanding of the structures and processes involved using the tools of density functional theory.

Macroscopic measurements on irradiated graphite reveal large strains (growth parallel to c-axis and contraction within the basal-planes), increases in thermal conductivity, various changes in mechanical properties (elastic constants, strength, creep behaviour), a drop in c-axis electrical resistivity, and an increase in internal energy. These are largely the result of lattice disorder and structural damage at the crystallite level due to isolated or partially aggregated submicroscopic defects, and depend to varying degrees on irradiation temperature, flux, dose and type of source[2,5–7]. Defect structure and behaviour in graphite/graphene has previously been modelled at various levels of theory[8–17], although largely semi-empirical, and not usually with the aim of understanding radiation effects. In fact, there remains substantial uncertainty as to even basic defect structure and individual defect roles in the development of damage and kinetics of energy release[5,18].

We have adopted a defect-in-supercell quantum-mechanical modelling scheme based on the formalism of density functional theory. This is implemented using a real-space gaussian orbital basis, pseudo-
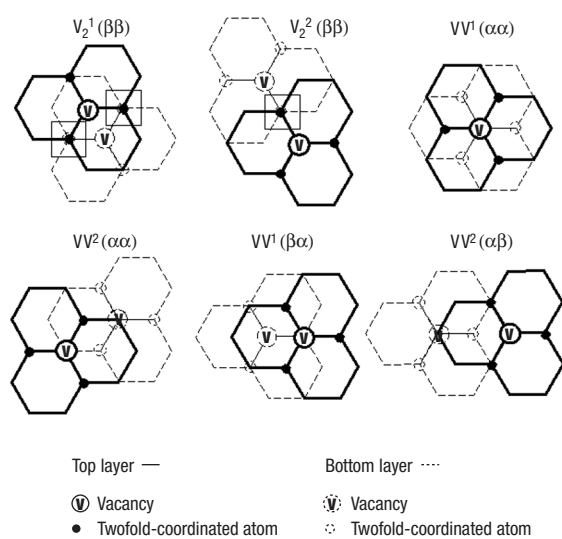
Figure 1 The zoo of close-proximity vacancies in adjacent layers in unsheared AB-stacked graphite. Only the $V_2^1(\beta\beta)$ (superscript 1 denotes first nearest interplane-neighbour; top left) and $V_2^2(\beta\beta)$ (superscript 2 denotes second nearest interplane-neighbour; top, centre) divacancy configurations allow bonding interactions between the twofold coordinated carbon atoms. Potential bonds are indicated by a square. In the $V_2^1(\beta\beta)$ case, only one of the possible interactions occurs, leaving the remaining two atoms surrounding each vacancy to form a weak reconstructed bond within the plane. The $\alpha\beta$ notation denotes vacant site type in the lower and upper layers (see text). The non-bonding configurations are denoted V V rather than V_2 for clarity.

potentials and a conjugate-gradient algorithm for optimization of atomic positions, and is described in detail elsewhere[19]. Cells used in these calculations were composed of 64 atoms in two layers that is, $4 \times 4 \times 1$ unit cells. Errors due to incomplete convergence with respect to basis, finite system size and Brillouin zone sampling, were estimated using trial defective and non-defective systems, and were typically much less than 0.4 eV of the converged value. However, we err on the side of caution with this value for our final results, because it also encompasses, and is representative of, the level of agreement/accuracy found between our calculation method (AIMPRO) and a reference plane-wave code (CASTEP)[20]. We present key defect calculations that shed new light on radiation damage behaviour, and show that a number of defect species form strong covalent bridges between atomic layers. Detailed results encompassing a greater part of the general damage scheme will appear in a series of forthcoming papers.

Atoms knocked from the graphite lattice by irradiation produce interstitial and vacancy defects, known as Frenkel pairs, and we begin our study with the vacancy. This is often assumed to be a planar defect, with essentially ideal, threefold symmetry[8,13,16]. However, in addition to an outward, symmetric breathing-mode relaxation, a Jahn–Teller distortion occurs, forcing a weak reconstructed bond between two of the surrounding carbons and displacing the third neighbour out of the atomic layer by about 0.7 Å (A. A. El-Barbary, R. H. Telling, C. P. Ewels, and M. I. Heggie, manuscript in preparation.). This and previous theoretical work suggests the Jahn–Teller distortion is essentially spontaneous, although in our case, the unstable equilibrium had to be perturbed and therefore we cannot rule out the existence of a small barrier <0.1 eV. The in-plane distortion is not great, but the vertical displacement is important in that it confers a greater propensity for out-of-plane interactions. In graphite, the vacancy can switch between the three symmetrically equivalent structures over a barrier of 0.1 eV—the

dynamic (~GHz at room temperature) superposition of which agrees with the symmetric experimental scanning tunnelling microscope (STM) images[21]. However, in the curved walls of a nanotube, the vacancy reconstruction would most likely favour the bond closest to being transverse to the axial direction. This picture of the distorted vacancy is also borne out in reference calculations made using a plane-wave code. Furthermore, the energies of formation and migration of the vacancy in our supercell, $E_f = 8.2$ eV and $E_m = 1.7$ eV respectively, are in broad agreement with previous theoretical work[13,14]. However, the large discrepancy between the theoretical (found from independent calculations[22]) and experimental migration energies, $E_m = 3.1 \pm 0.5$ eV, demands further attention. The widely used experimental value is derived from the kinetics of vacancy cluster growth in heavily irradiated, and therefore vacancy-rich graphite. In lightly irradiated graphite, evidence points towards a significantly lower migration barrier than is generally assumed (for example, ref. 23), also revealed by high vacancy mobility at surprisingly low temperatures[24].

To resolve this issue of vacancy transport in heavily irradiated graphite, we looked at the energetics of divacancies as candidates for the higher-energy activated process. A divacancy is formed when two neighbouring vacancies coalesce, the lowest energy state of which is when this occurs in the same atomic layer. This defect is planar with strongly reconstructed bonds enclosing two opposing fivefold rings, and a shared eightfold ring, $E_f = 8.7$ eV. However, E_m is ~7 eV, eliminating it from the frame, but to our surprise, a number of possible metastable divacancies can form when two vacancies approach one another in neighbouring sheets. We find that strong binding results from a shared covalent bond between the vertically displaced carbon atom associated with each vacancy; surprising given the undisturbed 3.35 Å interlayer distance. Examples of two interplanar divacancies formed in perfect AB-stacking are shown in Fig. 1. The participating vacancies are both of the β-type (ring centre above and below vacant lattice site), because in this configuration the displaced twofold coordinated atoms are sited one above the other, see Fig. 2. The first nearest interplane neighbour divacancy, $V_2^1(\beta\beta)$, is 1.9 eV more stable than two isolated vacancies, $E_f = 14.6$ eV, and the bridging bond is 1.43 Å in length. The second-nearest interplanar neighbour divacancy, $V_2^2(\beta\beta)$, is stabilized by a further 1.5 eV, $E_f = 13.0$ eV and with a slightly shorter bridging bond of 1.38 Å. The shared bond is less twisted in this symmetric geometry, allowing a double bond to form. In addition to the configurations given in Fig. 2, a range of other topological possibilities exist for interplanar divacancies in sheared graphite structures or multiwall nanotubes. For example, in AA-stacked graphite we find two stable divacancies, one with a single bond and the other with three single bonds. With respect to two isolated vacancies, these structures are lower in energy by 3.0 and 3.3 eV respectively.

Reference calculations made using a plane-wave code on the divacancy complexes $V_2^1(\beta\beta)$, $V_2^2(\beta\beta)$ found the difference in E_f was 1.4 eV, compared with the 1.5 eV found above using the gaussian basis code, and the same structures were obtained with crosslinking bond lengths of 1.44 and 1.38 Å respectively.

Crossplanar divacancies will act as traps that constrain vacancy migration, able to capture on two neighbouring planes, compared with the one plane for coplanar capture. Migration will then be controlled by de-trapping or movement between interplanar traps, resolving the discrepancy between theory and observation. On the assumption that vacancies will migrate by interconversion between $V_2^2(\beta\beta)$ and $V_2^1(\beta\beta)$, we add the formation energy difference between these two structures to the monovacancy migration energy, which is an estimate of the additional barrier for this process. This places the net barrier energy at 3.2 eV. Complete de-trapping from the $V_2^1(\beta\beta)$ defect, costing the binding energy of 1.9 eV plus E_m of 1.7 eV, would raise this barrier energy to 3.6 eV. In heavily irradiated graphites, mutual trapping will be expected to rate-limit or at least contribute to the overall transport process.
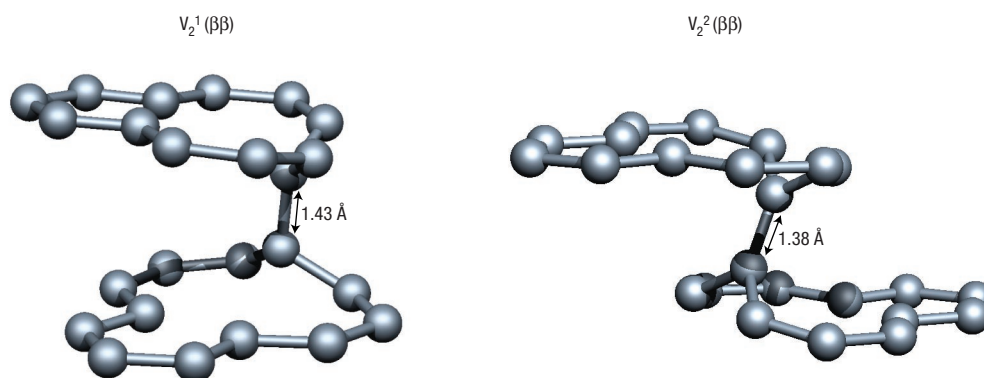
Figure 2 **The V$_2^1$(ββ) and V$_2^2$(ββ) interplanar divacancies.** The bridging bond lengths are 1.43 and 1.38 Å respectively, leaving the two remaining twofold coordinated atoms surrounding each vacancy to weakly reconstruct (bonds not shown) at 2.05 Å. Schematic of plan views are given in Fig. 1.

It is found that the graphite self-interstitial defect also tends to form crosslinks between the atomic layers. Previous work has shown that whilst in perfect graphite the interstitial sits above a bond centre, about half way between the layers, forming two covalent bonds, $E_f = 7.0$ eV, a more stable state is possible if the surrounding lattice is slightly sheared. A fourfold coordinated defect is now formed, Fig. 3, with a core similar to the spiropentane molecule[25]. We find that this shear-conferred stability is strong enough to spontaneously generate basal shift in a small supercell, where the cost of generating a stacking fault is modest in comparison with the localized bonding stability. The preferred basal shear is half a bond length in magnitude (0.71 Å) in a general bonding direction <1$\bar{1}$00>, see Fig. 4. When the shift direction is towards ABC stacking, the spiro-interstitial is favoured, $E_f = 5.5$ eV, and in the opposite direction, towards AA stacking, a threefold coordinated interstitial is favoured (with one vertical bond to the atom sited above), $E_f = 6.8$ eV. In the sheared supercells used here, both defects have lower formation energies compared with the grafted interstitial. Subtracting the double-stacking-fault cost (calculated in a defect-free cell) of $\gamma_{(3)} = 6.25$ and $\gamma_{(4)} = 2.13$ meV Å^{-2} respectively for the threefold and fourfold interstitial preferred stacking types, we can estimate the energy, E associated with the shear stability. With basal area $A = 82.64$ Å^2, we find $E \approx (E_{f\ 2\text{-bond}} - E_{f\ 3\text{-bond}}) + A\gamma_{(3)} = 0.7$ eV for the threefold interstitial, and $(E_{f\ 2\text{-bond}} - E_{f\ 4\text{-bond}}) + A\gamma_{(4)} = 1.7$ eV for the fourfold 'spiro' interstitial. In a graphite crystallite, as for a much larger supercell, we would not expect that such a shear would be nucleated spontaneously due to the prohibitive cost of generating fault (plus dislocation loop) over a large area, although this may be possible through a multidefect cooperative effect. Rather, we propose that these defects will be attracted to existing shear, such as exists within partial basal dislocations, present at very high densities in most graphite specimens[5] (up to approximately 10^{13}–10^{14} cm cm^{-3}) where the shift at the core is exactly **b**/2 = –0.71 Å (with reference to Fig. 4), where **b** is the Burgers vector. We propose that interstitial atoms will tend to lower their energy by segregating at the dislocation cores, having the effect of constraining their motion and interaction with other species along the dislocation line. Indeed, observations suggest that heterogeneous nucleation of interstitial aggregates does occur at the site of dislocations, although the mechanism for this was never clear[5]. These aggregates are believed to be important in c-axis dimensional change, and in Wigner energy release[18].

The recombination of interstitials and vacancies is expected to be the primary step in Wigner energy release, associated with a substantial 13–15 eV per pair, but despite various speculations as to the nature of this process and the possibility of a barrier, no substantive picture has emerged. On examining various approach routes for the interstitial, we find that a stable close-bound or intimate Frenkel pair defect, $E_f = 10.6$ eV, prevents the direct recombination route, posing a barrier of 1.4 eV that corresponds to its break-up. The interstitial adopts a threefold coordination at the edge of the vacancy, crosslinking to the next atomic layer, Fig. 5. The barrier is in good agreement with the experimental 1.38 ± 0.4 eV release barrier[26], assigned to the so-called 200 °C Wigner energy release peak. This prominent peak is observed in graphites irradiated below about 150 °C, and although it has been studied in detail, the defect species/process responsible remained undetermined, although di-interstitials have previously been implicated[7].

Unirradiated graphite typically has a high electrical resistivity, ρ_c, normal to the basal planes. However, defects that bind across the atomic layers can provide conduction paths in this direction, consistent with the observed drop in ρ_c post-irradiation[18]. This coupling between layers will also have an important effect on the passage of basal dislocations. Transmission electron microscopy has previously identified dislocation pinning by submicroscopic defects[27]. Measurements of the elastic constant associated with basal shear, c_{44}, pre- and post-irradiation also support this view. It is generally understood that in unirradiated graphite, reversible glide of basal dislocations confounds the intrinsic value of c_{44}, lowering it by up to an order of magnitude. After light irradiation, this dislocation motion is pinned and intrinsic c_{44} is measured[5].
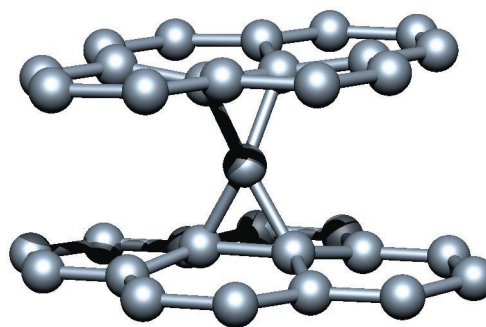

Figure 3 **The core atoms surrounding the fourfold coordinated 'spiro' interstitial, expected to exist within the core of basal dislocations.** Bond lengths ~1.49 Å, angles ~60 ± 2°.

Relative basal shift (Å)

−1.42   −0.71   0.00   0.71   1.42

ABC   ← AB →   AA

+0.05   +1.06   0.00   +3.13   +7.19
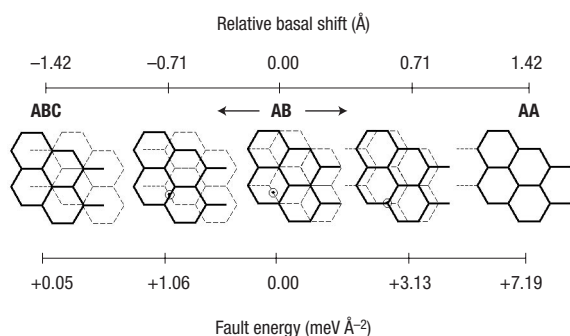
Fault energy (meV Å^{-2})

Figure 4 Schematic of stacking fault in graphite, showing relative shifts between layers and the corresponding perfect fault energy. The grafted interstitial sits in AB graphite above a bond centre, indicated by the circle. The spiro-interstitial forms when the stacking is −0.71 Å, taking up a position midway between layers above and below bond centres where the respective in-layer bonds eclipse at 120°, indicated by the circle. The threefold interstitial forms when the stacking is +0.71 Å, taking up a position above a bond centre with a vertical bond to an atom in the next layer, indicated by the circle. A basal dislocation core has stacking intermediate between AB and ABC, with the −0.71 Å structure at its centre. In a defect-free cell, single-layer shifts (double stacking fault) are essentially twice the perfect stacking fault energy.
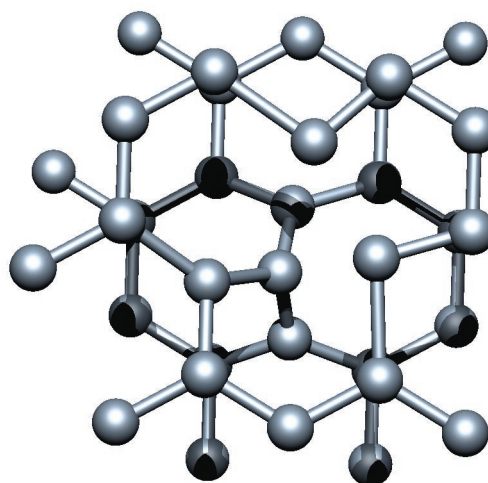
Figure 5 Plan view of the intimate Frenkel pair defect. The central threefold coordinated atom is the interstitial that sits below the vacancy in the top layer.

A principal difficulty with this explanation was in accepting that a point defect could pin the diffuse core of a basal dislocation.

However, our results show that crosslinking interstitials are stabilized at dislocation cores, and thus we expect they will pin dislocation motion by a barrier of up to 1.7 eV—the energy required to break the crosslinking bonds. Similarly, the intimate Frenkel pair and interplanar divacancy defects will also act as barriers to the passage of a dislocation. We assume that a large basal displacement, as would occur in the passage of a basal dislocation (1.42 Å for each partial), will break-up the structure. The energy costs associated with moving a 'free' dislocation in graphite are in the meV range over a micrometre-sized line segment. (Using anisotropic elasticity theory and a modified Peierls–Nabarro model[28], the core of a partial basal dislocation in graphite is found to be over 50 Å wide with a negligibly small Peierls energy barrier (10^{-8} eV Å^{-1}) and stress (10^{-16} Pa), due to the high in-plane stiffness (energy factor 0.44 eV Å^{-3} or 70 GPa) and low basal surface energy barrier (for **b**/2 = 0.71 Å, it is 1.06 meV Å^{-2}).) Therefore, an energy cost of 2–3 eV for defect break-up will act as a very effective barrier to further motion. These figures may overestimate the true strength, because metastable, half-broken structures may exist. Nevertheless, we expect the magnitude estimates hold, and we anticipate a strong pinning action. As the dislocation advances, this will ultimately result in the generation of Orowan loops of dislocation around the defect, in turn affecting the general evolution of microstructure and radiation creep behaviour[5].

Shear-stabilized defects will also pin small-angle twists and shears between graphite sheets during growth. We therefore suggest they will be important in determining final structure in turbostratic and disordered carbons, locking in stacking fault at an early stage. Such misorientation of the layer planes manifests as Moiré patterns—the so-called super-lattices observed in STM[29], in which 'islands' of AB- and AA-stacked graphite are surrounded by channels of intermediate stacking, such as that preferred by the interstitial. Other STM studies have provided the first tentative evidence for an association between point defects and large faults[30].

Bridging defects of the kind discussed here also seem to play an important role in multiwall nanotube structure and processes, including single-wall nanotube coalescence[31], molecular junction formation[32] and irradiation of nanotube bundles[17]. The structures we describe will act to increase axial shear resistance to sword-in-sheath failure mode[33], and also in nanotube joining processes, where vacancies are already believed to be the important species—the interplanar complexes discussed in this work provide a first-principles basis for the topology and energetics of the linking process.

Although the majority of our calculations were made using a spin-averaged functional, the reports of ferromagnetism in carbon structures and graphite[34] raise the tantalising possibility that spin-polarized states for these intrinsic point defects may be important in the origin of the effects. Our preliminary results on magnetic effects indicate that the ground state for the vacancy is a singlet state, but of greater interest in this context is evidence from our earlier work[25] for a highly mobile triplet state adatom (surface interstitial), with an energy very close to the singlet. We are currently extending these investigations to the interstitial in the bulk, that is, between layers, and although it is at this stage it is only possible to speculate, persistence of this triplet state could contribute to observed magnetization effects.

In summary, our understanding of a number of radiation effects in moderator graphite has been significantly advanced by a first-principles theoretical examination of point defect structure and behaviour, and the applicability of these findings extends to a range of important effects in related carbon materials. Although a theoretical study, we gain great confidence through the agreements we make with experiment and other calculations. Perhaps of greatest importance is our challenge to the common notion of vacancy defects confined to in-plane interactions. That we discover they can form complexes over the large interlayer distance—the graphite 'gap' was unexpected and in our view remarkable, and has helped us to understand vacancy transport.

References

1. Simmons, J. H. W. *Radiation Damage in Graphite* (Pergamon, London, 1965).
2. Arnold, L. *Windscale 1957: Anatomy of a Nuclear Accident* (Palgrave Macmillan, London, 1995).
3. Banhart, F. Irradiation effects in carbon nanostructures. *Rep. Prog. Phys.* **62**, 1181–1221 (1999).
4. Thrower, P. A. The study of defects in graphite by transmission electron microscopy. *Chem. Phys. Carbon* **5**, 217–319 (1969).
5. Kelly, B. T. *The Physics of Graphite* (Applied Science, London, 1981).
6. Kelly, B. T., Marsden, B. J. & Hall, K. *Irradiation Damage in Graphite due to Fast Neutrons in Fission and Fusion Systems* TECDOC-1154. (International Atomic Energy Agency, Vienna, Austria). Available online at http://www.iaea.org

7. Iwata, T. Fine structure of Wigner energy release spectrum in neutron-irradiated graphite. *J. Nucl. Mater.* **133-134,** 361–364 (1985).

8. Coulson, C. A. & Poole, M. D. Calculations of the formation energy of vacancies in graphite crystals. *Carbon* **2,** 275–279 (1964).

9. Thrower, P. A. & Loader, R. T. Interstitial atom energies in graphite. *Carbon* **7,** 467–477 (1969).

10. Nicholson, A. P. P. & Bacon, D. J. A defect molecule calculation for the vacancy in graphite. *Carbon* **13,** 275–282 (1975).

11. Zunger, A. & Englman, R. Self-consistent LCAO calculation of the electronic properties of graphite. II. Point vacancy in the two-dimensional crystal. *Phys. Rev. B.* **17,** 642–661 (1978).

12. Abrahamson, J. & Maclagan, G. A. R. Theoretical studies of interstitials in graphite. *Carbon* **22,** 291–295 (1984).

13. Kaxiras, E. & Pandey, K. C. Energetics of defects and diffusion mechanisms in graphite. *Phys. Rev. Lett.* **61,** 2693–2696 (1988).

14. Xu, C. H., Fu, C. L. & Pedraza, D. F. Simulations of point-defect properties in graphite by a tight-binding-force model. *Phys. Rev. B* **48,** 13273–13279 (1993).

15. Nordlund, K., Keinomen, J. & Mattila, T. Formation of ion irradiation induced small-scale defects on graphite surfaces. *Phys. Rev. Lett.* **77,** 699–702 (1996).

16. Hjort, M. & Stafström, S. Modeling vacancies in graphite via the Hückel method. *Phys. Rev. B* **61,** 14089–14094 (2000).

17. Salonen, E., Krasheninnikov, A. V. & Nordlund, K. Ion-irradiation-induced defects in bundles of carbon nanotubes. *Nucl. Instrum. Meth. B* **193,** 603–608 (2002).

18. Iwata, T., Nihira, T. & Matsuo, H. Irradiation and annealing effects on the *c*-axis electrical resistivity of graphite. *J. Phys. Soc. Japan* **36,** 123–129 (1974).

19. Coutinho, J., Jones, R., Briddon, P. R. & Öberg, S. Oxygen and dioxygen centers in Si and Ge: Density-functional calculations. *Phys. Rev. B* **62,** 10824–10840 (2000).

20. Payne, M. C., Teter, M. P., Allan, D. C., Aria, T. A. & Joannopoulos, J. D. Iterative minimization techniques for *ab initio* total-energy calculations: molecular dynamics and conjugate gradients. *Rev. Mod. Phys.* **64,** 1045–1097 (1992).

21. Kelly, K. F. & Halas, N. J. Determination of a and b site defects on graphite using C_{60}-adsorbed STM tips. *Surf. Sci.* **416,** L1085–L1089 (1998).

22. Thrower, P. A. & Mayer, R. M. Point defects and self-diffusion in graphite. *Phys. Status Solidi A* **47,** 11–37 (1978).

23. Asari, E., Kitajima, M., Nakamura, K. G. & Kawabe, T. Thermal relaxation of ion-irradiation damage in grapite. *Phys. Rev. B.* 47, 11143–11148 (1993).

24. Hinman, G. W., Haubold, A., Gardner, J. O. & Layton, J. K. Vacancies and interstitial clusters in irradiated graphite. *Carbon* **8,** 341–351 (1970).

25. Heggie, M. *et al.* LDF calculations of point defects in graphites and fullerenes. *Electrochem. Soc. Proc.* **98–8,** 60–67 (1997).

26. Mitchell, E. W. J. & Taylor M. R. Mechanism of stored-energy release at 200 °C in electron-irradiated graphite. *Nature* **208,** 638–641 (1965).

27. Grennal, A. Direct observations of dislocations in graphite. *Nature* **182,** 448–450 (1958).

28. Joós, B. & Duesbery, M. S. The Peierls stress of dislocations: An analytic formula. *Phys. Rev. Lett.* **78,** 266–269 (1997).

29. Xhie, J., Sattler, K., Ge, M. & Venkateswaran, N. Giant and supergiant lattices on graphite. *Phys. Rev. B.* **47,** 15835–15841 (1993).

30. Rong, Z. Y. Extended modifications of electronic structures caused by defects: Scanning tunneling microscopy of graphite. *Phys. Rev. B* **50,** 1839–1843 (1994).

31. Terrones, M., Terrones, H., Charlier, J. C., Banhart, F. & Ajayan, P. M. Coalescence of single-walled carbon nanotubes. *Science* **288,** 1226–1229 (2000).

32. Terrones M. *et al.* Molecular junctions by joining single-walled carbon nanotubes. *Phys. Rev. Lett.* **89,** 75505 (2002).

33. Yu M. F. *et al.* Strength and breaking mechanism of multiwalled carbon nanotubes under tensile load. *Science* **287,** 637–640 (2000).

34. Esquinazi, P. *et al.* Ferromagnetism in oriented graphite samples. *Phys. Rev. B* **66,** 024429 (2002).